Universal Dissipationless Dynamics in Gaussian Continuous-Variable Open Systems

Han-Jie Zhu,[1] Guo-Feng Zhang,[1,*] Lin Zhuang,[2] and Wu-Ming Liu[3,4,5]
[1]School of Physics and Nuclear Energy Engineering, Beihang University, Beijing 100191, China
[2]State Key Laboratory of Optoelectronic Materials and Technologies, School of Physics, Sun Yat-Sen University, Guangzhou 510275, China
[3]Beijing National Laboratory for Condensed Matter Physics, Institute of Physics, Chinese Academy of Sciences, Beijing 100190, China
[4]School of Physical Sciences, University of Chinese Academy of Sciences, Beijing 100190, China
[5]Songshan Lake Materials Laboratory, Dongguan, Guangdong 523808, China

(Received 9 May 2018; published 28 November 2018)

We investigate the universal dissipationless dynamics of Gaussian continuous-variable systems in the presence of a band-gapped bosonic environment. Our results show that environmental band gaps can induce localized modes, which give rise to the dissipationless dynamics where the system behaves as free oscillators instead of experiencing a full decay in the long-time limit. We present a complete characterization of localized modes and show the existence of the critical system-environment coupling. Beyond the critical values, localized modes can be produced, and the system dynamics become dissipationless. This novel dynamics can be utilized to overcome the environmental noises and protect the quantum resources in the continuous-variable quantum information.

DOI: 10.1103/PhysRevLett.121.220403

The dissipation and decoherence processes induced by surroundings are the central topic of study in the theory of open quantum systems. These unavoidable processes almost always lead to the irreversible loss of quantum coherence and quantum correlations, which are the crucial resources for quantum technologies [1–6]. Yet, quantum resources may be protected by utilizing quantum states that are less sensitive to environmental perturbations. This constitutes the basic idea of passive protection of quantum resources, which has been an important subject and had many applications in quantum information [7]. A prominent example is that of the decoherence-free subspaces, where the state evolution inside these subspaces is completely unitary [8–13]. Another novel example is the bound state, where the discrete eigenstate is formed inside the environmental band gap. Such a state is stable under environmental noise and gives rise to dissipationless dynamics when the non-Markovian effect is fully taken into account. For finite-dimensional systems such as spin systems, this phenomenon can occur for systems embedded in photonic band-gap materials, known as atom-photon bound states [14–26]. This feature can lead to many practical phenomena such as decoherence suppression [27], quantum entanglement and correlation preservation [28–33], quantum speedup [34], and metrology precision enhancement [35].

Despite significant progress on the subject, the analysis has almost exclusively been focused on few-body systems. The analogous behavior for many-body quantum systems is of general interest and highly desirable, since ultimately many schemes in practice require such systems. However, it is still a challenging and almost unexplored topic to understand such behavior in many-body systems. For another category of quantum systems, i.e., continuous-variable (CV) systems, another question arises: can bound states still be formed in the band-gapped environment, and if so, do these bound states lead to dissipationless dynamics? These questions are especially interesting for Gaussian systems, which constitute a large class of CV systems and play a central role, as well as serving as primary tools in CV quantum information. It would be novel and of practical relevance if bound states can be formed in Gaussian systems, which allows us to protect quantum resources in many CV protocols. Despite some previous papers that have addressed related simplified problems [36–42], the models discussed in these articles are small systems and can be regarded as finite-dimensional systems, since oscillators behave as few-level atoms in their invariant subspaces. Thus, these models may not provide correct bound-state properties in Gaussian systems, even for the single-oscillator case. Therefore, it is essential to establish a bound-state theory for general Gaussian systems.

In this Letter, we explore the Gaussian dissipationless dynamics in general CV systems with band-gapped bosonic environments and show that, differently from finite-dimensional systems, bound states in CV systems are characterized by localized modes with frequencies embedded in environmental spectral gaps. We obtain existence conditions of localized modes by analyzing non-Markovian dynamics, and our results confirm that these modes will give rise to dissipationless dynamics, where the system behaves as free oscillators in the long-time limit. As an important case, we analyze localized-mode properties in

the weak system-environment coupling limit which can be satisfied by most experimental settings. We further illustrate our results in an experimentally achievable system.

We consider that the system consists of N interacting oscillators bilinearly coupled to a general bosonic environment, as shown in Fig. 1(a). The total Hamiltonian can be written as $\hat{H} = \hat{H}_S + \hat{H}_E + \hat{H}_{int}$, where $\hat{H}_S = \boldsymbol{P}^T\boldsymbol{P}/2 + \boldsymbol{X}^T\boldsymbol{V}\boldsymbol{X}/2$ is the system Hamiltonian which describes N oscillators. The $N \times N$ matrix $\boldsymbol{V}$ defines the interaction between these oscillators, while column vectors $\boldsymbol{X} = (\hat{x}_1, \hat{x}_2, \ldots, \hat{x}_N)^T$ and $\boldsymbol{P} = (\hat{p}_1, \hat{p}_2, \ldots, \hat{p}_N)^T$ store coordinates and momenta of oscillators. The environment contains M bosonic reservoirs and is described by the Hamiltonian $\hat{H}_E = \sum_\alpha \hat{H}^{(\alpha)}$ with $\hat{H}^{(\alpha)} = \sum_k (\hat{p}_k^{(\alpha)2} + \omega_k^2 \hat{q}_k^{(\alpha)2})/2$. The interaction Hamiltonian is $\hat{H}_{int} = \sum_{\alpha i k} C_{ik}^{(\alpha)} \hat{x}_i \hat{q}_k^{(\alpha)} = \boldsymbol{X}^T \sum_\alpha \boldsymbol{C}^{(\alpha)} \boldsymbol{Q}^{(\alpha)}$, where each oscillator can simultaneously interact with many reservoirs, and $C_{ik}^{(\alpha)}$ is the coupling between the ith oscillator and mode k in the reservoir α. This interaction is relevant in many realistic scenarios, where the oscillator is coupled principally to one reservoir and weakly to others. We emphasize that this model describes a general linear network of open oscillators and can appear in various physical systems [40,43–47], as well as model most Gaussian protocols in the CV quantum information [48,49].

The state of N oscillators can be completely described by the characteristic function defined as $\chi(\boldsymbol{k}, t) = \mathrm{Tr}[\rho(t)\hat{D}(\boldsymbol{k})]$. Here $\hat{D}(\boldsymbol{k}) = \exp[i(\boldsymbol{X}^T\boldsymbol{k}_x - \boldsymbol{P}^T\boldsymbol{k}_p)]$ is the Weyl operator, and $\boldsymbol{k} = (\boldsymbol{k}_x, \boldsymbol{k}_p)$ is a $2N$-component vector in the phase space [48–50]. In this work, we focus on Gaussian dynamics and assume the initial state of the total system to be factorized, while each reservoir $H^{(\alpha)}$ has a thermal initial state with temperature $T^{(\alpha)}$. Then, the state evolution can be obtained by using the path-integral method with the Feynman-Vernon influence functional [51], and it satisfies [52]

$$\chi(\boldsymbol{k}, t) = \chi[\boldsymbol{\Phi}(t)\boldsymbol{k}, 0] \exp\left[-\frac{1}{2}\boldsymbol{k}^T\boldsymbol{\Sigma}(t)\boldsymbol{k} + i\Pi^T(t)\boldsymbol{k}\right], \quad (1)$$

where the transition matrix $\boldsymbol{\Phi}(t)$ and thermal covariance matrix $\boldsymbol{\Sigma}(t)$ are $2N \times 2N$ matrices, and $\Pi(t)$ is a $2N$ vector. These coefficients are determined by the Green function matrix $\boldsymbol{G}(t)$ of the system, which satisfies

$$\ddot{\boldsymbol{G}}(t) + \boldsymbol{V}\boldsymbol{G}(t) - 2(\boldsymbol{\eta} * \boldsymbol{G})(t) = 0 \quad (2)$$

with initial conditions $\boldsymbol{G}(0) = 0$ and $\dot{\boldsymbol{G}}(0) = \boldsymbol{I}$, where the symbol $*$ denotes the time convolution, i.e., $(A * B)(t) = \int_0^t d\tau A(t-\tau)B(\tau)$. Here $\boldsymbol{\eta}(t) = \int d\omega \boldsymbol{I}(\omega) \sin\omega t$ is the dissipation kernel dependent on the environmental spectral density $\boldsymbol{I}(\omega)$, where $\boldsymbol{I}(\omega) = \sum_\alpha \boldsymbol{I}^{(\alpha)}(\omega)$ and $\boldsymbol{I}^{(\alpha)}(\omega) = \sum_k \boldsymbol{C}_k^{(\alpha)T}\boldsymbol{C}_k^{(\alpha)}\delta(\omega - \omega_k)/(2m_k\omega_k)$. In this model, coefficients in Eq. (1) are given by $\boldsymbol{\Pi}(t) = 0$, $\boldsymbol{\Phi}(t) = \begin{pmatrix} \dot{\boldsymbol{G}}(t) & \boldsymbol{G}(t) \\ \ddot{\boldsymbol{G}}(t) & \dot{\boldsymbol{G}}(t) \end{pmatrix}$, and $\boldsymbol{\Sigma}(t) = \begin{pmatrix} \boldsymbol{\sigma}^{(0,0)}(t) & \boldsymbol{\sigma}^{(0,1)}(t) \\ \boldsymbol{\sigma}^{(1,0)}(t) & \boldsymbol{\sigma}^{(1,1)}(t) \end{pmatrix}$, where matrices $\boldsymbol{\sigma}^{(n,m)}$ are determined by $\boldsymbol{\sigma}^{(n,m)}(t) = \int_0^t dt_1 \int_0^t dt_2 \boldsymbol{G}^{(n)}(t_1)\boldsymbol{\nu}(t_1 - t_2)\boldsymbol{G}^{(m)}(t_2)$ and the noise kernel $\boldsymbol{\nu}(t) = \sum_\alpha \int d\omega \boldsymbol{I}^{(\alpha)}(\omega) \coth(\omega/2k_BT_\alpha)\cos(\omega t)$ [52].

Existence conditions of localized modes.—We search for conditions that maintain the Green function $\boldsymbol{G}(t)$, since dissipationless dynamics will appear if the Green function $\boldsymbol{G}(t)$ shows a nonvanishing behavior; otherwise, the system would experience a full decay, as seen from Eq. (1). Without loss of generality, we assume the coupling strength can be written as $C_{ik}^{(\alpha)} = gC_{ik}^{\prime(\alpha)}$, where g is the global coupling strength and $C_{ik}^{\prime(\alpha)}$ describes the local microscopic details. Meanwhile, we consider the environmental spectrum that contains a gap between 0 and ω_c, i.e., the spectral density $\boldsymbol{I}(\omega) = \boldsymbol{0}$ when ω is inside the gap [Fig. 1(b)]. Such a band-gapped spectrum can be achieved by utilizing the environment engineering, e.g., photonic crystals [53–56]. Results of other spectrums can also be obtained with small modifications to our theory.

The matrix $\boldsymbol{G}(t)$ can be solved using the Laplace transform, and we find $\tilde{\boldsymbol{G}}(s) = [s^2\boldsymbol{I} + \boldsymbol{V} - 2\tilde{\boldsymbol{\eta}}(s)]^{-1}$, where the notation $\tilde{f}$ is used to denote the Laplace transformation of the function f. We introduce the eigenvalue function $\lambda_k(s, g)(k = 1, 2, \ldots, N)$, which denotes the kth eigenvalue

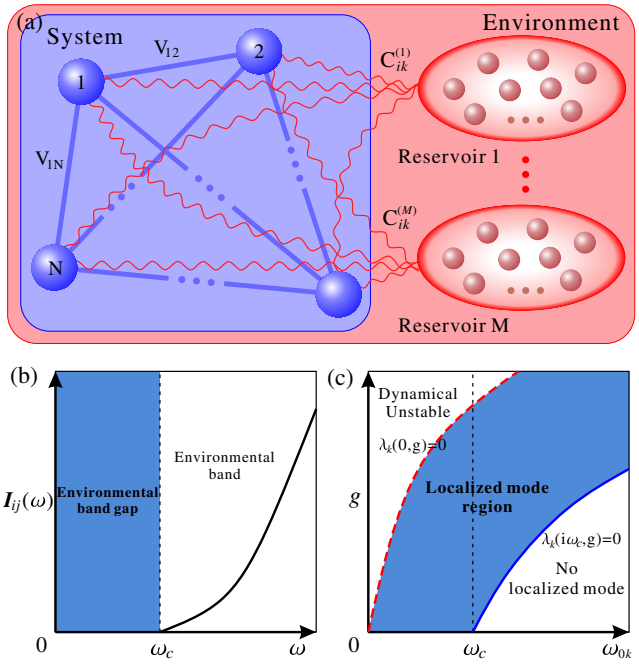

FIG. 1. (a) Illustration of the general Gaussian network of open oscillators. Here N interacting oscillators (blue spheres) are bilinearly coupled with bosonic reservoirs, while each reservoir consists of different noninteracting bosonic modes (red spheres). (b) Band-gapped structure of the environment spectrum. (c) Localized mode status. The kth localized mode presents above the critical coupling line (blue solid line). Meanwhile, the system becomes dynamically unstable in the regime that fails to meet the stability condition (above the red dashed line).

of $\tilde{\boldsymbol{G}}^{-1}(s,g)=s^2\boldsymbol{I}+\boldsymbol{V}-2g^2\tilde{\boldsymbol{\eta}}'(s)$. Here $\tilde{\boldsymbol{\eta}}(s)=g^2\tilde{\boldsymbol{\eta}}'(s)$. The order of eigenvalues can be defined by using the eigendecomposition $\tilde{\boldsymbol{G}}^{-1}(s,g)=\boldsymbol{U}(s,g)\boldsymbol{\Lambda}(s,g)\boldsymbol{U}^{+}(s,g)$, where we fix the order of eigenvalues for a specific s_0, g_0 and require that both $\Lambda(s,g)$ and $\boldsymbol{U}(s,g)$ be continuous for s and g. This creates correspondences of eigenvalues between different s's and g's. Under this definition, the function $\lambda_k(iy,g)$ is monotonically decreasing for both $y\in(0,\omega_c)$ and g, while $\lambda_k(x,g)$ is monotonically increasing for $x\geq 0$ [57]. We note that the condition $\lambda_k(0,g)>0$ should be satisfied by physical systems which can be properly described by the model in Fig. 1(a). If $\lambda_k(0,g)<0$ for specific k, a real singular point will present and give rise to the divergent behavior in $\boldsymbol{G}(t)$. Physically, as we will show later, a mode with imaginary frequency appears when $\lambda_k(0,g)<0$. Thus, the total Hamiltonian has no ground state, and the system will tend towards a state with infinite negative energy. In this case, the model is dynamically unstable and should be corrected to avoid this unphysical feature by including terms previously neglected, e.g., the nonlinear term. Outside this unstable region, if we have $\lambda_k(i\omega_c,g)<0$, there must be one root ω_{sk} such that $\lambda_k(i\omega_{sk},g)=0$. This root is related to an imaginary singular point of $\tilde{\boldsymbol{G}}(s)$, which produces a nondecay oscillation in $\boldsymbol{G}(t)$ with frequency ω_{sk}, and thus associates with dissipationless dynamics.

In fact, each imaginary singular point corresponds to a localized mode with frequency inside the spectral gap. This can be confirmed by diagonalizing the Hamiltonian into a set of normal modes, where these modes are combinations of oscillator modes and bath modes, and their position operators have the form $\boldsymbol{X}'=\boldsymbol{u}^{(0)}\boldsymbol{X}+\sum_\alpha \boldsymbol{u}^{(\alpha)}\boldsymbol{Q}^{(\alpha)}$. The lth column $\boldsymbol{u}_l^{(0)}$ of the matrix $\boldsymbol{u}^{(0)}$ is determined by the secular equation $(\boldsymbol{V}-\sum_\alpha \boldsymbol{C}^{(\alpha)T}\boldsymbol{V}_l^{(\alpha)-1}\boldsymbol{C}^{(\alpha)})\boldsymbol{u}_l^{(0)T}=\omega_l^2\boldsymbol{u}_l^{(0)T}$, where $(\boldsymbol{V}_l^{(\alpha)})_{jk}=(\omega_l^2-\omega_k^2)\delta_{jk}$ and ω_l is the lth normal mode frequency [57]. This equation is equivalent to $\tilde{\boldsymbol{G}}^{-1}(i\omega_l)\boldsymbol{u}_l^{(0)T}=\boldsymbol{0}$; thus the singular point $i\omega_{sk}$ creates a localized mode with frequency ω_{sk}. This result is quite different from the bound-state behavior in finite-dimensional systems, where only bound states in low-excitation subspaces can be calculated, and dissipationless dynamics are only understood in the zero-temperature case. For Gaussian systems, bound states in the whole Hilbert space can be completely determined, and they form localized modes which behave as free oscillators. During the dissipation process, a significant amount of photons remain in localized modes, while others dissipate into the environment and, thus give dissipationless dynamics regardless of the reservoir temperature.

Based on the above discussions, we can now formulate existence conditions of localized modes. First, if all reservoirs are neglected, the system behaves as N independent effective oscillators with effective frequencies $\omega_{0k}(k=1,\ldots,N)$ given by square roots of eigenvalues of the coupling matrix $\boldsymbol{V}$. If the frequency ω_{0k} is inside the gap $(0,\omega_c)$, then the eigenvalue function $\lambda_k(iy,g)$ will possess a zero in $(0,\omega_c)$, since $\lambda_k(i\omega_{0k},g)<\lambda_k(i\omega_{0k},0)=0$; thus the kth localized mode appears for arbitrary coupling g. Secondly, if the frequency ω_{0k} is outside the gap $(0,\omega_c)$, there always exists a nonzero critical coupling g_{ck} which satisfies $\lambda_k(i\omega_c,g_{ck})=0$. The corresponding localized mode presents when the coupling strength g exceeds the critical value g_{ck} [Fig. 1(c)].

Localized modes and dissipationless behavior.—We next focus on the system dynamics. When the system-reservoir coupling is below the smallest critical coupling, no localized mode can present, and the system experiences a complete decay. In this case, the matrix $\tilde{\boldsymbol{G}}(s)$ has no poles, and we have

$$\boldsymbol{G}(t)=\boldsymbol{\mathcal{I}}(t)=-\frac{i}{\pi}\int_{\omega_c}^{\infty}dy\,\sin yt[\boldsymbol{M}(y)-\boldsymbol{M}^{+}(y)],\quad(3)$$

where $\boldsymbol{M}(y)$ is a $N\times N$ matrix. Here we assume that the spectral density behaves as $\boldsymbol{I}(\omega)\sim(\omega-\omega_c)^\alpha$, $\omega\to\omega_c$; then the transient function $\boldsymbol{\mathcal{I}}(t)$ vanishes as $O(t^{-1-\alpha})$ [58]. Consequently, the transition matrix becomes zero, and the thermal covariance matrix evolves to asymptotic values determined by reservoirs. The initial distribution finally disappears, and the system reaches thermal equilibrium with the environment.

Localized modes appear when the coupling strength is above the corresponding critical coupling. By including poles of $\tilde{\boldsymbol{G}}(s)$, we obtain $\boldsymbol{G}(t)$ as

$$\boldsymbol{G}(t)=\boldsymbol{\Omega}(t)+\boldsymbol{\mathcal{I}}(t),\quad \boldsymbol{\Omega}(t)=\sum_k\boldsymbol{\Omega}_k\frac{\gamma_k}{\omega_{sk}}\sin\omega_{sk}t.\quad(4)$$

Here, $\boldsymbol{\Omega}(t)$ is the undamped oscillating term associated with localized modes, where $\boldsymbol{\Omega}_k$ is the $N\times N$ rank-1 projection matrix, and the coefficient γ_k is the residue that characterizes the amplitude of the kth localized mode. The coefficient γ_k is nonzero if and only if the coupling g is above the critical coupling g_{ck}. Over long times, the transient function $\boldsymbol{\mathcal{I}}(t)$ vanishes, and only the undamped oscillation $\boldsymbol{\Omega}(t)$ remains. Thus, the system dynamics in the long-time limit can be described as

$$\begin{aligned}\boldsymbol{\Phi}(t)&\sim\sum_k\frac{\gamma_k}{\omega_{sk}}\begin{pmatrix}\omega_{sk}\cos\omega_{sk}t & \sin\omega_{sk}t\\ -\omega_{sk}^2\sin\omega_{sk}t & \omega_{sk}\cos\omega_{sk}t\end{pmatrix}\otimes\boldsymbol{\Omega}_k,\\ \boldsymbol{\Sigma}(t)&\sim\boldsymbol{\Sigma}_0+\sum_{j,k}\boldsymbol{\Sigma}_{j,k}(t)+\sum_{j\neq k}\boldsymbol{\Sigma}_{j,-k}(t),\end{aligned}\quad(5)$$

where $\boldsymbol{\Sigma}_{j,\pm k}(t)=\boldsymbol{\Sigma}_{j,\pm k}^{(0)}\exp[i(\omega_{sj}\pm\omega_{sk})t]+\text{H.c.}$, and $\boldsymbol{\Sigma}_0$ and $\boldsymbol{\Sigma}_{j,\pm k}^{(0)}$ are time-independent coefficients. Exact forms of coefficients $\boldsymbol{M}(y)$, $\boldsymbol{\Omega}_k$, γ_k, $\boldsymbol{\Sigma}_0$, and $\boldsymbol{\Sigma}_{j,\pm k}^{(0)}$ are given in the Supplemental Material [57].

The above results show that localized modes give rise to dissipationless dynamics. Each presented localized mode contributes a periodic rotation in the phase space, which is similar to the free evolution of the Wigner function. Moreover, the thermal covariance matrix $\mathbf{\Sigma}(t)$ no longer reaches an asymptotic value but oscillates with various frequencies due to the interference between localized modes. This implies that the system is far from equilibrium even in the long-time limit.

The weak-coupling limit.—For the weak-coupling case, where the oscillator-reservoir coupling is weak compared to the effective frequency, such that $g \ll \omega_{0k}$, the reservoir contribution $-2\tilde{\boldsymbol{\eta}}(s)$ in $\boldsymbol{G}^{-1}(s)$ can be viewed as a small term so that the perturbation method can be applied. The coupling matrix $\boldsymbol{V}$ can be diagonalized as $\boldsymbol{V}_d = \boldsymbol{P}\boldsymbol{V}\boldsymbol{P}^{+}$, where $\boldsymbol{P}$ is a unitary matrix and $(\boldsymbol{V}_d)_{jk} = \omega_{0k}^2\delta_{jk}$. Then we have $\tilde{\boldsymbol{G}}_d^{-1}(iy, g) = -y^2\boldsymbol{I} + \boldsymbol{V}_d - 2g^2\tilde{\boldsymbol{\eta}}_d'(iy)$, where $\tilde{\boldsymbol{G}}_d^{-1} = \boldsymbol{P}\tilde{\boldsymbol{G}}^{-1}\boldsymbol{P}^{+}$ and $\tilde{\boldsymbol{\eta}}_d' = \boldsymbol{P}\tilde{\boldsymbol{\eta}}'^{-1}\boldsymbol{P}^{+}$. In the nondegenerate case, such that $g \ll |\omega_{sj} - \omega_{sk}|$ for $j \neq k$, we can obtain first-order corrections of eigenvalue functions as $\lambda_k(iy, g) = -y^2 + \omega_{0k}^2 - 2g^2\tilde{\eta}_{dkk}'(iy)$. This allows us to obtain localized mode frequencies and critical couplings as

$$\omega_{sk}^2 = \omega_{0k}^2 - g^2\tilde{\eta}_{dkk}'(i\omega_{0k}) + O(g^4) \quad (\omega_{0k} < \omega_c),$$
$$g_{ck}^2 = \frac{\omega_{0k}^2 - \omega_c^2}{2\tilde{\eta}_{dkk}'(i\omega_c)}\theta(\omega_{0k} - \omega_c) + O((\omega_{0k}^2 - \omega_c^2)^2). \tag{6}$$

A clear physical picture can be drawn from this: (i) The localized mode frequency ω_{sk} is the effective frequency ω_{0k} plus a negative shift of order $O(g)$, and (ii) the critical coupling increases as $\omega_{0k} - \omega_c$ when ω_{0k} is above and near the band edge. Moreover, we can find that $\gamma_k = 1 + O(g^2)$ and $\boldsymbol{U}(i\omega_{sk}) = \boldsymbol{I} + O(g^2)$ when $\omega_{0k} < \omega_c$. Thus, the decay process is prohibited, and the system is completely isolated from the environment in the weak-coupling limit if all effective frequencies are inside the gap. This is in contrast to the usual situations, where Markovian dynamics become *dominating* and the system experiences the exponential decay.

Cavities in waveguides.—To illustrate our results, we now present an example of a system with a band-gapped environment. Such a system can be experimentally realized in an array of coupled cavities, which are synthesized in optical waveguides [59–68]. Here, each cavity $H_{\mathrm{S}n} = \omega_0 a_n^{+} a_n$ is linearly coupled to a waveguide $H_{\mathrm{E}n} = \sum_k \omega_k b_{nk}^{+} b_{nk}$, which consists of an array of linear defects. For simplicity, we assume that both cavities and waveguides are identical. The interaction Hamiltonian is $H_{\mathrm{I}n} = \sum_k g_k(a_n^{+} + a_n)(b_{nk}^{+} + b_{nk})$, with $\omega_k = \omega_1 - 2\kappa\cos kx_0$ and $g_k = \kappa_0 \sin kx_0$, where ω_1 is the frequency of linear defects, x_0 and κ are the spatial separation and the hopping rate between adjacent defects, respectively [39,69]. The coefficient κ_0 describes the coupling strength between the cavity and its adjacent defect. In the tight-binding approximation, we also consider the interaction $\alpha\omega_0(a_n^{+} + a_n)(a_{n\pm1}^{+} + a_{n\pm1})$ between adjacent cavities $H_{\mathrm{S}n}$ and $H_{\mathrm{S}(n\pm1)}$, and the interaction $\beta\sum_k g_k(a_n^{+} + a_n)(b_{(n\pm1)k}^{+} b_{(n\pm1)k})$ between the cavity $H_{\mathrm{S}n}$ and its adjacent waveguides $H_{\mathrm{E}(n\pm1)}$, where α and β are the relative coupling strengths. One can notice that the spectrum of waveguides shows upper and lower frequency limits, and there are two continuous gaps outside the energy band. Each gap can produce a group of localized modes, and their existence is determined by the matrices $\tilde{\boldsymbol{G}}^{-1}[i(\omega_1 + 2\kappa)]$ and $\tilde{\boldsymbol{G}}^{-1}[i(\omega_1 - 2\kappa)]$, respectively. In Fig. 2(a), we show the localized mode status which agrees with our previous discussions clearly. An unstable region exists in the upper-left portion, and its extent is decided by $\tilde{\boldsymbol{G}}^{-1}(0)$. Below this unstable region, the kth localized mode always exists if the effective frequency ω_{0k} is inside the environment band gap $(0, \omega_0 - 2\kappa)$ or $(\omega_0 + 2\kappa, +\infty)$. Moreover, there exists a critical coupling line for each localized mode, which appears above this line.

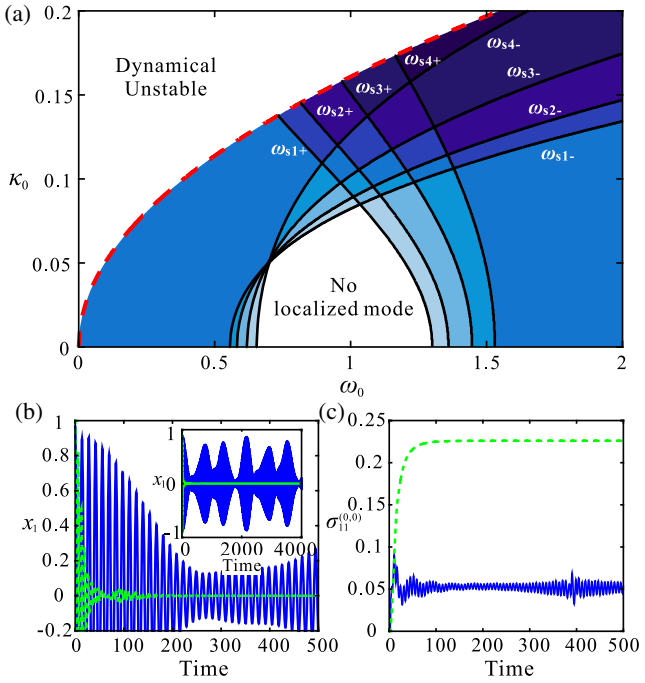

FIG. 2. (a) Localized mode status of cavities in optical waveguides. Each critical coupling line is labeled with the corresponding mode frequency $\omega_{sk\pm}$, where the sign $\pm$ indicates that the localized mode is inside the band gap $(\omega_1 + 2\kappa, \infty)$ or $(0, \omega_1 - 2\kappa)$. Localized modes can exist in the region above their corresponding critical coupling lines. (b) Time evolution of the expectation $\langle\hat{x}_1\rangle$. (c) Time evolution of the element $\sigma_{11}^{(0,0)}$ of the thermal covariance matrix. In panels (b) and (c), blue solid lines (green dashed lines) correspond to the circumstance where localized modes are present (absent), with $\kappa_0 = 0.05$ and $\omega_0 = 0.5$ ($\omega_0 = 1$). The first cavity is initially in the coherent state $|\alpha\rangle$, $\alpha = 1$, while others are in vacuum states. All reservoirs have vacuum initial states. In all panels, the system consists of four cavities, while other parameters chosen are $\omega_1 = 1$, $\kappa_0 = 0.05$, $\kappa = 0.2$, $\alpha = 0.2$, and $\beta = 0.2$.

The system dynamics is shown in Figs. 2(b) and 2(c). Clearly, when localized modes present, the system experiences a partial decay and becomes dissipationless after a long time. In Fig. 2(b), the time evolution of $\langle \hat{x}_1 \rangle$ can be described as the superposition of different periodic oscillations. This indicates that in the long-time limit, the system behaves as the combination of several periodic rotations in the phase space, and each rotation corresponds to a localized mode. Besides, Fig. 2(c) shows that the system fails to reach the equilibrium with the environment; instead, there exist periodic energy flows between them.

Experimentally, localized modes can be produced by slightly detuning the cavity frequency ω_0 from the defect frequency ω_1 by changing the geometrical parameters of cavities. Since the waveguide has a very narrow band, a small detuning is enough to insure the cavity frequency inside the band gap. For example, in the coupled-cavity system in photonic crystal slabs, the typical frequencies of defects and hopping rate are $\omega_1 = 0.305 \times 2\pi c/d$ and $\kappa = 1.5 \times 10^{-3} \times 2\pi c/d$, where d is the lattice period [70]. In order to probe the dynamics, we can directly measure photon currents flowing over waveguides. These photon currents describe the tunneling of photons between cavities and waveguides, and will oscillate persistently if localized modes present; otherwise, they will disappear rapidly, since the system will reach equilibrium with the environment in a very short time. Therefore, dissipationless dynamics can be confirmed by the observation of nonvanishing oscillating photon currents.

Conclusion.—In summary, we have presented a general theory of the dissipationless dynamics for open Gaussian systems, and shown that dissipationless dynamics is a universal feature for Gaussian systems with band-gapped environments. This novel dynamics arises from localized modes, which are formed as long as effective frequencies of oscillators are inside the environmental spectrum gap or the system-environment coupling exceeds the critical values. Such a feature allows us to suppress environmental noises by modifying the environment in order to induce localized modes. Our theory can be applied to most Gaussian CV protocols and sheds light on the way to protect quantum resources in the CV quantum information. It also provides a clue to understanding the non-Markovianity in more general many-body open quantum systems.

This work was supported by the NSFC under Grants No. 11574022, No. 11434015, No. 61227902, No. 61835013, No. 61775242; the National Key R&D Program of China under Grant No. 2016YFA0301500; and the Strategic Priority Research Program of the Chinese Academy of Sciences under Grants No. XDB01020300 and XDB21030300.

H. J. Z. and G. F. Z. contributed equally to this work.

*gf1978zhang@buaa.edu.cn

[1] I. de Vega and D. Alonso, Rev. Mod. Phys. **89**, 015001 (2017).
[2] I. Buluta, S. Ashhab, and F. Nori, Rep. Prog. Phys. **74**, 104401 (2011).
[3] C. L. Degen, F. Reinhard, and P. Cappellaro, Rev. Mod. Phys. **89**, 035002 (2017).
[4] X. Gu, A. F. Kockum, A. Miranowicz, Y. X. Liu, and F. Nori, Phys. Rep. **718–719**, 1 (2017).
[5] J. Q. You and F. Nori, Nature (London) **474**, 589 (2011).
[6] B. M. Garraway and H. Perrin, J. Phys. B **49**, 172001 (2016).
[7] D. Suter and G. A. Álvarez, Rev. Mod. Phys. **88**, 041001 (2016).
[8] P. Zanardi and M. Rasetti, Phys. Rev. Lett. **79**, 3306 (1997).
[9] D. Kielpinski, V. Meyer, M. A. Rowe, C. A. Sackett, W. M. Itano, C. Monroe, and D. J. Wineland, Science **291**, 1013 (2001).
[10] J. Q. You, X. Hu, and F. Nori, Phys. Rev. B **72**, 144529 (2005).
[11] W. Qin, C. Wang, and X. Zhang, Phys. Rev. A **91**, 042303 (2015).
[12] P. Z. Zhao, G. F. Xu, Q. M. Ding, E. Sjöqvist, and D. M. Tong, Phys. Rev. A **95**, 062310 (2017).
[13] A. F. Kockum, G. Johansson, and F. Nori, Phys. Rev. Lett. **120**, 140404 (2018).
[14] S. John and J. Wang, Phys. Rev. Lett. **64**, 2418 (1990).
[15] S. John and T. Quang, Phys. Rev. A **50**, 1764 (1994).
[16] H. B. Liu, J. H. An, C. Chen, Q. J. Tong, H. G. Luo, and C. H. Oh, Phys. Rev. A **87**, 052139 (2013).
[17] F. Giraldi, Phys. Rev. A **91**, 062112 (2015).
[18] H. Z. Shen, X. Q. Shao, G. C. Wang, X. L. Zhao, and X. X. Yi, Phys. Rev. E **93**, 012107 (2016).
[19] E. Sanchez-Burillo, D. Zueco, J. J. Garcia-Ripoll, and L. Martin-Moreno, Phys. Rev. Lett. **113**, 263604 (2014).
[20] M. F. Maghrebi and A. V. Gorshkov, Phys. Rev. B **93**, 014307 (2016).
[21] Y. Wu, J. Wang, and H. Zhang, Opt. Commun. **366**, 431 (2016).
[22] T. Shi, Y. H. Wu, A. González-Tudela, and J. I. Cirac, Phys. Rev. X **6**, 021027 (2016).
[23] P. T. Fong and C. K. Law, Phys. Rev. A **96**, 023842 (2017).
[24] C. J. Yang and J. H. An, Phys. Rev. B **95**, 161408 (2017).
[25] G. Calajó, F. Ciccarello, D. Chang, and P. Rabl, Phys. Rev. A **93**, 033833 (2016).
[26] S. Yang, M. Al-Amri, S. Y. Zhu, and M. S. Zubairy, Phys. Rev. A **87**, 033818 (2013).
[27] Q. Tong, J. An, H. Luo, and C. H. Oh, J. Phys. B **43**, 155501 (2010).
[28] Q. J. Tong, J. H. An, H. G. Luo, and C. H. Oh, Phys. Rev. A **81**, 052330 (2010).
[29] C. Lazarou, K. Luoma, S. Maniscalco, J. Piilo, and B. M. Garraway, Phys. Rev. A **86**, 012331 (2012).
[30] W. L. Yang, J. H. An, C. Zhang, M. Feng, and C. H. Oh, Phys. Rev. A **87**, 022312 (2013).
[31] L. J. Feng, Y. J. Zhang, G. C. Xing, Y. J. Xia, and S. Q. Gong, Ann. Phys. (Amsterdam) **377**, 77 (2017).
[32] P. Facchi, M. S. Kim, S. Pascazio, F. V. Pepe, D. Pomarico, and T. Tufarelli, Phys. Rev. A **94**, 043839 (2016).

[33] J. Cheng, W. Z. Zhang, Y. Han, and L. Zhou, Phys. Rev. A **91**, 022328 (2015).
[34] H. B. Liu, W. L. Yang, J. H. An, and Z. Y. Xu, Phys. Rev. A **93**, 020105 (2016).
[35] Y. S. Wang, C. Chen, and J. H. An, New J. Phys. **19**, 113019 (2017).
[36] C. J. Yang, J. H. An, H. G. Luo, Y. Li, and C. H. Oh, Phys. Rev. E **90**, 022122 (2014).
[37] J. H. An and W. M. Zhang, Phys. Rev. A **76**, 042127 (2007).
[38] M. Wu, C. U. Lei, W. Zhang, and H. Xiong, Opt. Express **18**, 18407 (2010).
[39] E. Sánchez-Burillo, D. Zueco, L. Martín-Moreno, and J. J. García-Ripoll, Phys. Rev. A **96**, 023831 (2017).
[40] D. Boyanovsky and D. Jasnow, Phys. Rev. A **96**, 012103 (2017).
[41] Y. Lin, P. Yang, and W. Zhang, Sci. Rep. **6**, 34804 (2016).
[42] W. M. Zhang, P. Y. Lo, H. N. Xiong, M. Wei-Yuan Tu, and F. Nori, Phys. Rev. Lett. **109**, 170402 (2012).
[43] X. Zhou, I. Dotsenko, B. Peaudecerf, T. Rybarczyk, C. Sayrin, S. Gleyzes, J. M. Raimond, M. Brune, and S. Haroche, Phys. Rev. Lett. **108**, 243602 (2012).
[44] M. Aspelmeyer, T. J. Kippenberg, and F. Marquardt, Rev. Mod. Phys. **86**, 1391 (2014).
[45] K. Hammerer, M. Aspelmeyer, E. S. Polzik, and P. Zoller, Phys. Rev. Lett. **102**, 020501 (2009).
[46] T. Opatrný, Phys. Rev. Lett. **119**, 010502 (2017).
[47] Q. Sun, X. H. Hu, W. M. Liu, X. C. Xie, and A. C. Ji, Phys. Rev. A **84**, 023822 (2011).
[48] S. L. Braunstein and P. van Loock, Rev. Mod. Phys. **77**, 513 (2005).
[49] C. Weedbrook, S. Pirandola, R. García-Patrón, N. J. Cerf, T. C. Ralph, J. H. Shapiro, and S. Lloyd, Rev. Mod. Phys. **84**, 621 (2012).
[50] R. Simon, N. Mukunda, and B. Dutta, Phys. Rev. A **49**, 1567 (1994).
[51] R. P. Feynman and F. L. Vernon, Ann. Phys. (N.Y.) **24**, 118 (1963).
[52] E. A. Martinez and J. P. Paz, Phys. Rev. Lett. **110**, 130406 (2013).
[53] C. F. Fong, Y. Ota, S. Iwamoto, and Y. Arakawa, Phys. Rev. B **95**, 245423 (2017).
[54] G. Calajò, L. Rizzuto, and R. Passante, Phys. Rev. A **96**, 023802 (2017).
[55] Y. Liu and A. Houck, Nat. Phys. **13**, 48 (2016).
[56] R. Ooi and Q. Gong, J. Appl. Phys. **110**, 063513 (2011).
[57] See Supplemental Material at http://link.aps.org/supplemental/10.1103/PhysRevLett.121.220403 for detailed derivations and explicit expressions of related coefficients.
[58] R. Wong, *Asymptotic Approximations of Integrals* (Society for Industrial and Applied Mathematics, Philadelphia, 2001).
[59] M. Bayindir, B. Temelkuran, and E. Ozbay, Phys. Rev. Lett. **84**, 2140 (2000).
[60] M. Verbin, O. Zilberberg, Y. E. Kraus, Y. Lahini, and Y. Silberberg, Phys. Rev. Lett. **110**, 076403 (2013).
[61] M. C. Rechtsman, J. M. Zeuner, Y. Plotnik, Y. Lumer, M. Segev, and A. Szameit, Nature (London) **496**, 196 (2013).
[62] J. Lu, L. Zhou, L. M. Kuang, and F. Nori, Phys. Rev. A **89**, 013805 (2014).
[63] J. Q. Liao, Z. R. Gong, L. Zhou, Y. X. Liu, C. P. Sun, and F. Nori, Phys. Rev. A **81**, 042304 (2010).
[64] L. Zhou, Z. R. Gong, Y. X. Liu, C. P. Sun, and F. Nori, Phys. Rev. Lett. **101**, 100501 (2008).
[65] D. Leykam, B. A. Malomed, and A. S. Desyatnikov, J. Opt. **15**, 044016 (2013).
[66] Y. C. Zhang, X. F. Zhou, X. Zhou, G. C. Guo, H. Pu, and Z. W. Zhou, Phys. Rev. A **91**, 043633 (2015).
[67] H. Leblond, D. Kremer, and D. Mihalache, Phys. Rev. A **95**, 043839 (2017).
[68] G. Masada, K. Miyata, A. Politi, T. Hashimoto, J. L. Obrien, and A. Furusawa, Nat. Photonics **9**, 316 (2015).
[69] S. Longhi, Phys. Rev. B **80**, 165125 (2009).
[70] D. P. Fussell and M. M. Dignam, Appl. Phys. Lett. **90**, 183121 (2007).